Proceedings of Proceedings of ASME Turbo Expo 2016: Turbomachinery Technical Conference and Exposition
GT2016
June 14-June 17, 2016, Seoul, South Korea

GT2016-58016

STUDY OF THE WALL THERMAL CONDITION EFFECT IN A LEAN-PREMIXED DOWNSCALED CAN COMBUSTOR USING LARGE-EDDY SIMULATION

D. Mira[*], **M. Vázquez, G. Houzeaux**
CASE Department
BSC-CNS
Barcelona, Spain
Email: daniel.mira@bsc.es

S. Gövert, J.W.B. Kok
Thermal Engineering Department
University of Twente
Enschede, Netherlands

E.I. Mahiques[†], **L. Panek**
Siemens AG
Power Generation
10553 Berlin - Germany

ABSTRACT

The primary purpose of this study is to evaluate the ability of LES, with a turbulent combustion model based on steady flamelets, to predict the flame stabilization mechanisms in an industrial can combustor at full load conditions. The test case corresponds to the downscaled Siemens can combustor tested in the high pressure rig at the DLR. The effects of the wall temperature on the prediction capabilities of the codes is investigated by imposing several heat transfer conditions at the pilot and chamber walls. The codes used for this work are Alya and OpenFOAM, which are well established CFD codes in the fluid mechanics community. Prior to the simulation, results for 1-D laminar flames at the operating conditions of the combustor are compared with the detailed solutions. Subsequently, results from both codes at the mid-plane are compared against the experimental data available. Acceptable results are obtained for the axial velocity, while discrepancies are more evident for the mixture fraction and the temperature, particularly with Alya. However, both codes showed that the heat losses influence the size and length of the pilot and main flame.

NOMENCLATURE

CFD Computational Fluid Dynamics
RANS Reynolds-averaged Navier-Stokes
LES Large-eddy simulation
FGM Flame-Generated Manifolds
HPC High-Performance Computing
RPV Reaction progress variable
CSP Computational Singular Perturbation
ER Equivalence ratio

INTRODUCTION

The design of modern combustion systems needs to address several challenges in aspects related to reduction of pollutant emissions using lean mixtures, increment in flexibility of operation and avoiding thermo-acoustic instabilities [**?**, **?**, **?**]. The use of numerical simulations as a tool for the design of combustion systems is growing in the last decade as more computing power is becoming available. The enhancement of numerical methods and physical models in CFD codes contributes to the reduction in costs of research and development, although many challenges are still to be faced [**?**]. The existence of heat losses in modern gas turbines is also an important aspect when modelling combustion applications. The heat losses influence not only the formation of pollutants, but also the dynamics of the flow and eventually the stabilization of the flames [**?**, **?**]. While the mixture fraction does not change significantly due to heat losses, the temperature is usually reduced at the walls because of the cooling. Therefore, low enthalpy mixture is expected near the walls. This affects the thermochemical as well as the transport properties of the fluid in this region, but also influences the flow field in the rest of

[*]Address all correspondence to this author: daniel.mira@bsc.es
[†]PhD Student University of Twente

the chamber due to the flow recirculation created to stabilize the flame. Accounting for these effects can improve the prediction of the numerical simulations and can provide further insights into the physics of the system.

The present study is focused on the modelling of the reacting flow field on a downscaled can combustor using LES and evaluate the effects of heat losses on the flow dynamics. The test case corresponds to a downscaled can combustor of the DLR, which has been previously investigated experimentally [?]. Experimental data is available for part and full load at different operating conditions, although the numerical simulation will be focused on the full load condition at 4 bar with preheated air and 1.2 MW thermal power burning pure methane. The combustor consists of a main burner with 8 swirling injectors and a central conical-shaped pilot burner. Further details of the geometry can be found in the work by Lückerath et al. [?]. This combustor has already been investigated numerically by Goldin et al. [**?**] in adiabatic conditions using RANS and LES providing acceptable correlation with the experimental data when using the FGM combustion model. The present work aims to evaluate the same operating point, but investigates the effect of heat losses on the prediction capabilities of the codes. The heat losses are accounted for by imposing several heat transfer conditions at the wall chamber and the cone walls, where the flame is anchored to the pilot. Due to the strong interaction between the pilot and the main regions, this thermal condition is expected to affect the position where the flame stabilizes at both the wall chamber and the cone. Consequently, the final results will be affected by the different thermal conditions applied and the differences will be quantified.

The numerical simulations will be conducted with two different codes Alya [**?**] and OpenFOAM [**?**], which are well-established CFD codes in the fluid mechanics community. Alya is a parallel multi-physics CFD code of the PRACE Benchmark Suite for HPC applications and uses the finite element method. OpenFOAM is a CFD code used for turbomachinery applications, well-known in the community and uses the finite-volume method. Both codes are updated with a turbulent combustion model based on steady flamelets. While the combustion model in Alya uses a flamelet database based on premixed flamelets with transport properties and source terms tabulated [?], OpenFOAM uses a tabulation based on the source term of the reaction progress variable [**?**].

The paper is organized as follows. Firstly, the numerical methods, LES and combustion model of the two codes are presented. Secondly, the two codes are compared on a 1-D premixed flame configuration at different mixture fractions operating at the same conditions as the combustor. Finally, results of the downscaled can combustor using LES in adiabatic and non-adiabatic conditions are presented. Analysis of the results and the effects of heat losses on the interaction between the central pilot flame and the main burners are discussed.

MODELLING APPROACH

The numerical simulations presented on this study are based on solving the Navier-Stokes equations for reacting flows in the context of LES. The filtered governing equations include the continuity, momentum and total enthalpy along with transport equations for the filtered reaction progress variable $\tilde{c}$ and mixture fraction $\tilde{f}$. Details of the combustion models and numerical methods are now provided.

CFD codes

The code Alya uses a spatial discretization based on the Finite Element method using the Variational Multiscale Stabilization technique [**?**] and the subgrid scale effects are accounted for by the WALE model [**?**]. A second-order Crank-Nicholson time integration scheme is used for the LES simulations.

For the OpenFOAM simulations [?], the second order limitedLinear scheme is used for the divergence terms. Linear schemes are used for the laplacian and gradient terms. A blended Crank-Nicholson scheme, with a blend factor of 0.5, is used for the temporal terms. The pimple loop is employed to solve the equations, with 4 outer correctors and 3 inner pressure correctors. The one equation eddy viscosity model is selected as the subgrid turbulence model.

Chemistry tabulation

OpenFOAM

One-dimensional flamelets are obtained using the GRI 3.0 kinetic mechanism in the Cantera software. The variables used for the generation of the 3-D table are the progress variable, the mixture fraction and the total enthalpy. Only the source terms of the progress variable are tabulated, so that a compact table is obtained. The progress variable is based on the CO_2 mass fraction:

$$c = \frac{Y_{CO_2}}{Y_{CO_2,\mathrm{eq}}} \tag{1}$$

The mixture fraction is a conserved scalar of the fuel fraction and the total enthalpy includes the chemical enthalpy. The CFD solver takes the source term obtained from the tables, based on the local values of the CO_2 mass fraction, mixture fraction and enthalpy. Consequently, a transport equation is solved for each of those variables. The relevant species mass fractions (i.e. reactants and combustion products) are calculated from the following

1-step reaction:

$$CH_4 + \frac{2}{ER}O_2 + \frac{2}{ER}\frac{1-\chi_{O_2}}{\chi_{O_2}}N_2 = \quad (2)$$

$$\alpha CO_2 + \beta CO + \gamma H_2O + \mu O_2 + \nu H_2 + \frac{2}{ER}\frac{1-\chi_{O_2}}{\chi_{O_2}}N_2 \quad (3)$$

where χ_{O_2} is the mole fraction of oxygen in air and ER refers to the equivalence ratio. From the balance equations for the atoms C, H and O, an analytical solution for each of the species mass fraction can be obtained. Further details of this combustion model can be found in [?].

Alya

The non-premixed database is generated from laminar premixed flamelets using the code PREMIX [**?**]. The creation of the manifolds $\phi(f,c)$ differs depending on the flammability region. While outside flammability limits, mixture averaged properties are used, laminar premixed flamelets obtained with PREMIX are generated for each value of mixture fraction. The definition of the progress variable is based on the CSP method, which obtains the b-vector that weights the contribution of each species on the reaction progress variable [?]. The definition of the RPV is given by:

$$\eta = \sum_{k=1}^{N} b_k Y_k \quad (4)$$

$$c = \frac{\eta - \eta^u}{\eta^b - \eta^u} \quad (5)$$

where N is the total number of species used by the GRI 3.0 mechanism and the subscripts u and b reference the unburnt and burnt mixture respectively. The use of the CSP approach results into a more uniform distribution of the source term along the span of the reaction progress variable allowing larger time-steps and reducing the stiffness of the chemistry calculation [?].

RESULTS AND DISCUSSION

The results of the simulations are presented in this section. A description of the test case is introduced, followed by the comparison of the combustion models at the investigated operating point in a 1D configuration. Details of the mesh for the full geometry are provided along with the comparison of the numerical results with the experimental data. Discussion on key physical phenomena is also discussed.

Experimental test case

The burner consists of eight main swirl burners arranged on an annulus with a pilot swirl burner at the center. The fuel staging uses two fuel lines, which directly inject into the swirling vanes of the main and pilot burners. The combustor also includes an ignition burner that was also considered in the simulations. The length of the combustion chamber is 380 mm, while a rectangular cross section of 95x95 mm^2 double-glassed windows with air cooling are used for the combustion chamber walls. The combustion air is preheated up to 704 K, while cold fuel is injected at a temperature of about 363 K. The numerical simulations will consider the conditions of the combustor operated at p = 4 bar with a maximum thermal load of 1.2 MW. The conditions imposed at each of the boundaries are summarized in Table 1 and an sketch of the combustor is given in Fig. 1.

TABLE 1: Conditions imposed at the inlet and outlet patches.

	$Main_{air,in}$	$Main_{fuel,in}$	$Pilot_{air,in}$	$Pilot_{fuel,in}$	Outlet
T (K)	704	363	704	553	-
$\dot{m}$ (g/s)	636.3	19.9	70.7	2.71	-
f	0	1	0	1	-
P (bar)	-	-	-	-	4

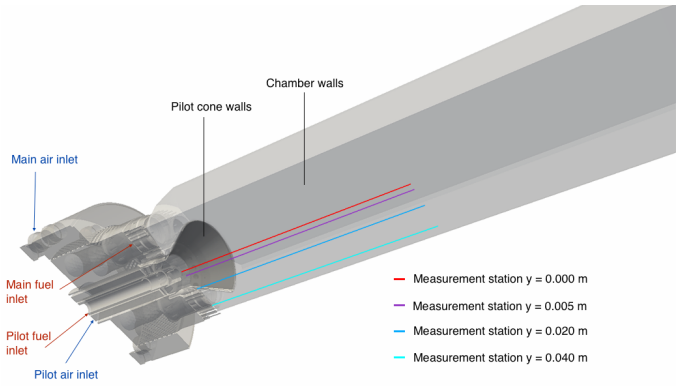

FIGURE 1: GEOMETRY AND COMPUTATIONAL BOUNDARIES.

1D flames at full load conditions

Before conducting the LES simulation of the full combustor, the codes are compared at the operating point of the combustor in a 1D premixed flame configuration. The results of the flames at different equivalence ratios with the corresponding temperature after mixing are shown in Fig.2. These results are used as a verification of the chemical database and its correct integration into the CFD codes. Besides, the solution fields of the 1D flames also provide information about the chemical structure of the flames that will be predicted by the simulations.

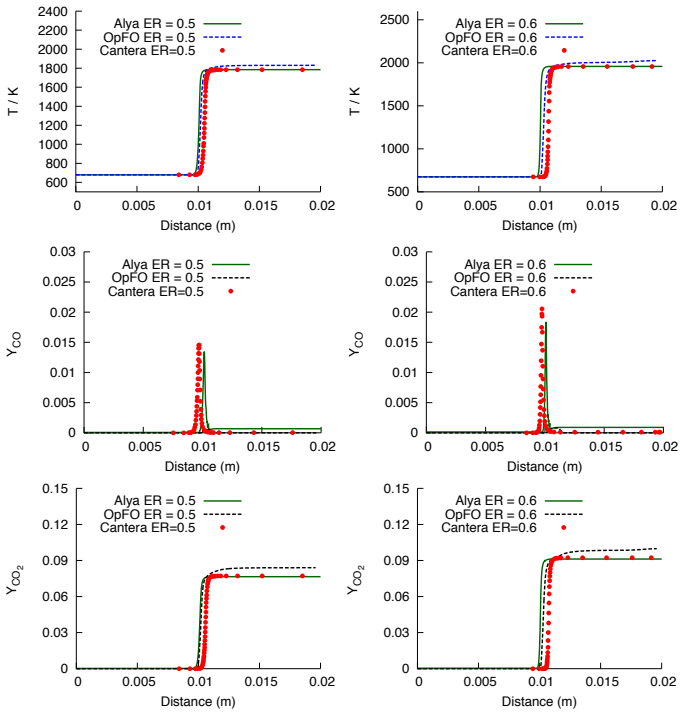

FIGURE 2: TEMPERATURE AND SPECIES MASS FRACTIONS AT TWO EQUIVALENCE RATIOS.

The results show good correlation when compared to the reference solution provided by Cantera. The PREMIX solution is not shown here in order to allow an easy comparison taking Cantera as a reference solution. It is observed a slight over-prediction of the equilibrium temperature for the OpenFOAM code that does not occur in Alya, which is capable of reproducing the Cantera adiabatic flame temperature. In the case of the species, the differences between the two codes become more evident. The same trend is observed for the prediction of CO_2, where OpenFOAM slightly over-predicts the mass fraction. The results indicate differences for the prediction of CO between PREMIX and Cantera. In particular, PREMIX generates a chemical structure where part of CO was not oxidized to CO_2, while Cantera assumes a full oxidation for the CO. The formation of CO occurs very rapidly on a small length scale, and the peak values differ between the two codes. OpenFOAM is not able predict the CO formation because CO is calculated from the CO_2 mass fraction, and the combustion model can only predict CO at equilibrium conditions.

Simulation setup

The computational mesh employed by Alya to solve the problem is composed by 47 million tetrahedrons and has been refined along the multi-perforated plates as well as the central pilot and the surrounding burners, where the swirlers are located. The

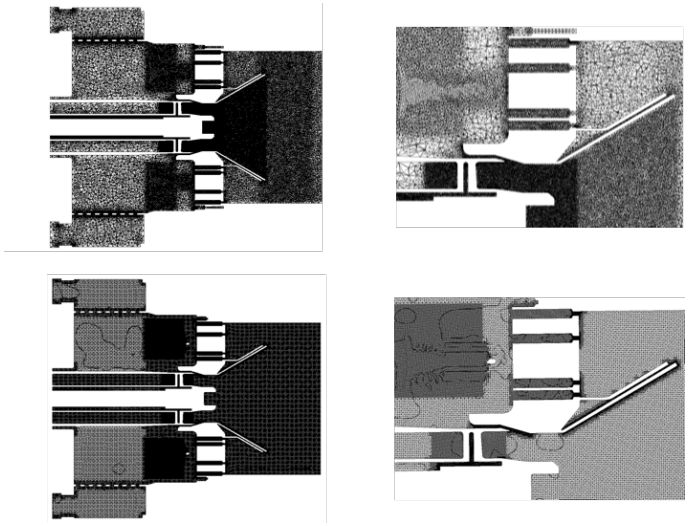

FIGURE 3: Z-PLANE OF THE COMPUTATIONAL MESHES: ALYA (TOP) AND OPENFOAM(BOTTOM).

mesh used in OpenFOAM has about 32 million cells: 30 million hexahedrons, 1.5 million polyhedrons, 0.5 million prisms and few tetrahedrons. It was not possible to use this mesh with Alya due to the incompatibility of the polyhedrons with the finite element method, while numerical issues occurred when running OpenFOAM with the full tetrahedron mesh. Details of these meshes can be seen in Fig. 3. A zoom region of the piloted injection and main burners can be distinguished on the right-hand side plot of Fig. 3 for both grids.

The numerical investigation is focused on the effects of the wall temperature on the development of the flow field and the prediction capabilities of the codes. Several thermal conditions are imposed at the walls of the combustion chamber to evaluate the cooling effects on the flame dynamics. The approach (1) considers an adiabatic condition where the heat flux is zero $q = -k\nabla \mathrm{T} = 0$. The approach (2) considers an isothermal condition imposed as a constant wall temperature: T_w=1500K at the cone walls and T_w=1000K at combustion chamber walls, while the approach (3) assumes adiabatic walls at the cone, but isothermal walls at T_w=1000K for the combustion chamber. A summary of the test cases is shown in Table 2. The boundary conditions and the measurement locations where the comparison with the experimental data takes place is shown in Fig. 1. The experimental data available for comparison is given at three radial positions and along the streamwise direction of the combustor. The axial values for mixture fraction and temperature correspond to $y = 0, 20, 34$ mm, while the experimental data for the axial velocity is given at $y = 0, 20, 39$ mm respectively.

TABLE 2: TEST CASES AND THERMAL BOUNDARY CONDITIONS.

Name	Walls chamber	Walls pilot
Adiab.	$q = 0$	$q = 0$
Isotherm.(1)	T_w = 1000K	T_w = 1500K
Isotherm.(2)	T_w = 1000K	$q = 0$

Numerical results

Numerical simulations using LES have been conducted with the two codes for the configuration shown in Fig. 1. The combustor operates in the lean regime with equivalence ratio around $ER = 0.55$. The flame is stabilized in the burner along the prolongation of the central cone walls with the surrounding burner. The flame is anchored in this region because of the wake of the pilot cone, but also due to the addition of the air that is employed for cooling pilot cone. This results in a zone with high enthalpy, which promotes a higher flame speed when the hot air is mixed with the fuel. The LES results are time-averaged for three residence times and mean values for velocity, temperature and mixture fraction are compared with the experimental data from Lückerath et al. [?].

As only thermal conditions for the walls are varied, the qualitative results for the velocity and mixture fraction are quite similar for the three cases. Time-averaged results of the axial velocity for the two codes are shown in Fig. 4 for comparison. The first discrepancy between the codes is at the main air inflow, since Alya predicts a higher velocity of the flow before passing the perforated plates. Although the flow through the swirlers was not compared, the axial velocities at the end of the pilot cone are in good agreement. The same can be stated for the air in the pilot passage. The length and width of the recirculation zone predicted by the two codes are comparable, although Alya predicts a stronger recirculation than OpenFOAM. The axial velocity predicted by Alya at the rear of the chamber is significantly higher than the one computed by OpenFOAM. The reason for this discrepancy can be seen in Fig 5, where the time-averaged mixture fraction is shown. The mixture fraction field is an important quantity that defines the distribution of fuel/air mixture in the combustor and, together with the enthalpy provides the thermal state of the system. In general, a uniform mixture fraction is predicted inside the chamber except at the pilot cone region, where it is sensibly higher in order to stabilize the combustor. When comparing the solutions, Alya predicts a higher mixture fraction than OpenFOAM. This produces a higher temperature due to the combustion of a richer mixture, which results in the velocity difference shown in Fig. 4.

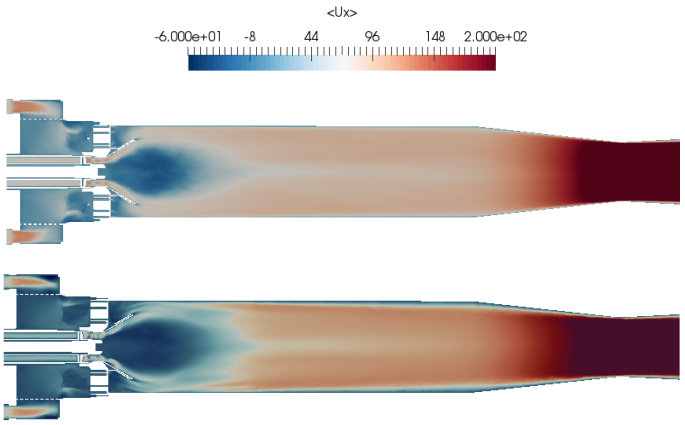

FIGURE 4: TIME-AVERAGED AXIAL VELOCITY AT MIDDLE PLANE FOR *OPENFOAM* (TOP) AND *ALYA* (BOTTOM) FOR THE ISOTHERM.(1) CASE.

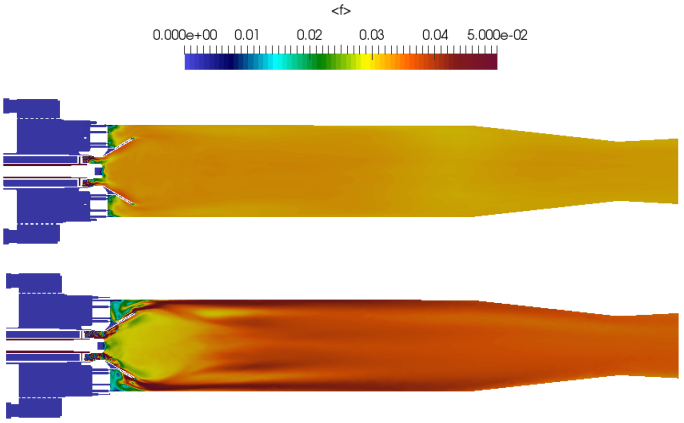

FIGURE 5: TIME-AVERAGED MIXTURE FRACTION AT MIDDLE PLANE FOR *OPENFOAM* (TOP) AND *ALYA* (BOTTOM) FOR THE ISOTHERM.(1) CASE.

The predicted axial velocity of the codes on the measurement lines for the different thermal conditions is shown in Figs. 6 and 7 for Alya and OpenFOAM respectively. The comparison indicates a good level correlation near the centreline of the combustor for both codes, while some discrepancies appear as the flow approaches the combustor walls. The size of the central recirculation zone is well predicted by the codes, although both codes over-predict the strength of the recirculation resulting in a larger reverse velocity. This difference can be attributed to the presence of the igniter and the momentum exchanged by this injection and the interaction with the flow of the pilot. The last plot at $y = 0.039$m located within the annulus region also indicates that the codes cannot capture the thin boundary layer formed over the

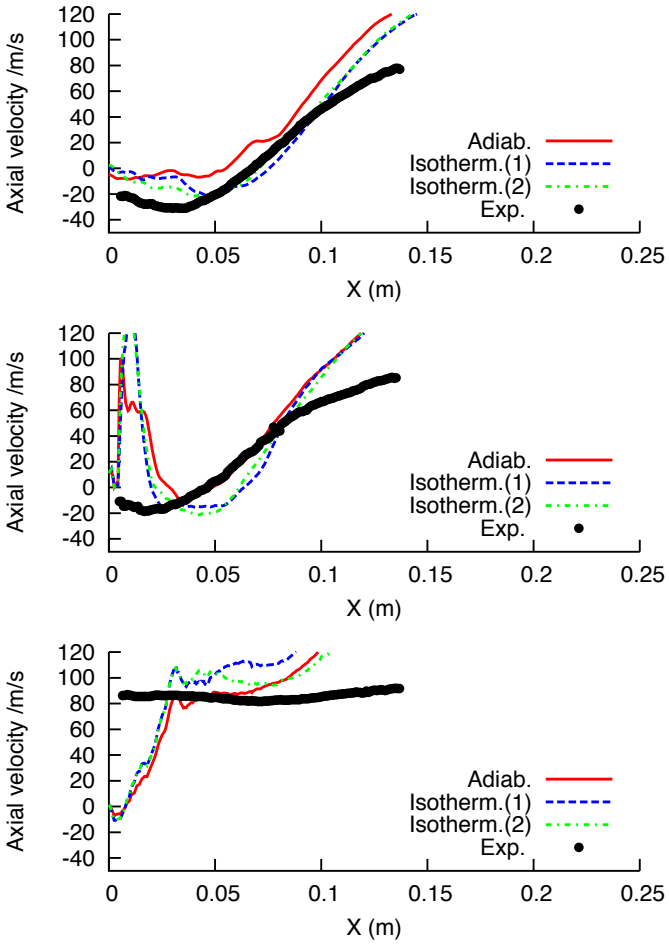

FIGURE 6: ALYA: AXIAL VELOCITY COMPARISON WITH EXPERIMENTAL DATA AT y=0.005m (TOP), y=0.020m (MIDDLE) and y=0.039m (BOTTOM).

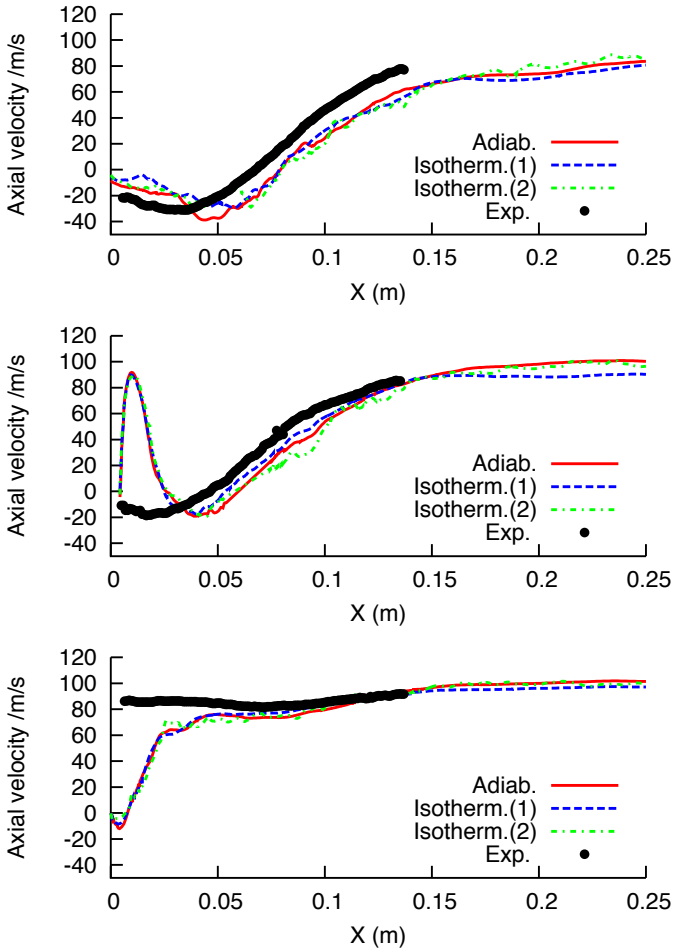

FIGURE 7: OPENFOAM: AXIAL VELOCITY COMPARISON WITH EXPERIMENTAL DATA AT y=0.005m (TOP), y=0.02m (MIDDLE) and y=0.039m (BOTTOM).

cone walls of the central part of the combustor.

Comparison of the two codes at the prediction of the mixture fraction are shown in Figs. 8 and 9. The figures show a good level of correlation between OpenFOAM and the experimental data at the three measurement locations. The comparison reveals an over-prediction of the mean mixture fraction in Alya that becomes more evident in the external part of central annulus. In particular, there is a region close to the cone walls where the mixture fraction is very high and transported by the velocity near the wall leading to a mixture fraction peak at x=0.015 m. In the case of OpenFOAM, the correlation with the experiments is better and it is only at the upstream locations where the prediction is not satisfactory. The combustor develops a rich jet on the inside of the nozzle cone that is under-predicted by OpenFOAM and over-predicted in Alya. This over-prediction causes the combustor to operate near stoichiometric conditions and therefore, at higher temperature for Alya. The effects of heat losses also influence the temperature field in the entire combustion chamber, as shown in Figs. 10 and 11, but to a much less extent. Particularly, in both codes the same effect is observed: from the adiabatic case to the isothermal (1) case, the main flame gets shorter, the pilot flame lengthens slightly and the main temperature in the chamber remains almost invariant. The temperature field for the isothermal (2) case, which presents a pilot flame similar to the adiabatic case, does not differ much from the isothermal (1) case because the isothermal temperature imposed at the walls (1500 K) is close to the adiabatic flame temperature. Therefore, the main sources of heat loss are can be attributed to the chamber walls.

Due to the over-prediction of mixture fraction in Alya, the equivalence ratio rises above the stoichiometric condition at the exit of the combustor where the flame is anchored and an over-prediction of the temperature is expected in this region. This can

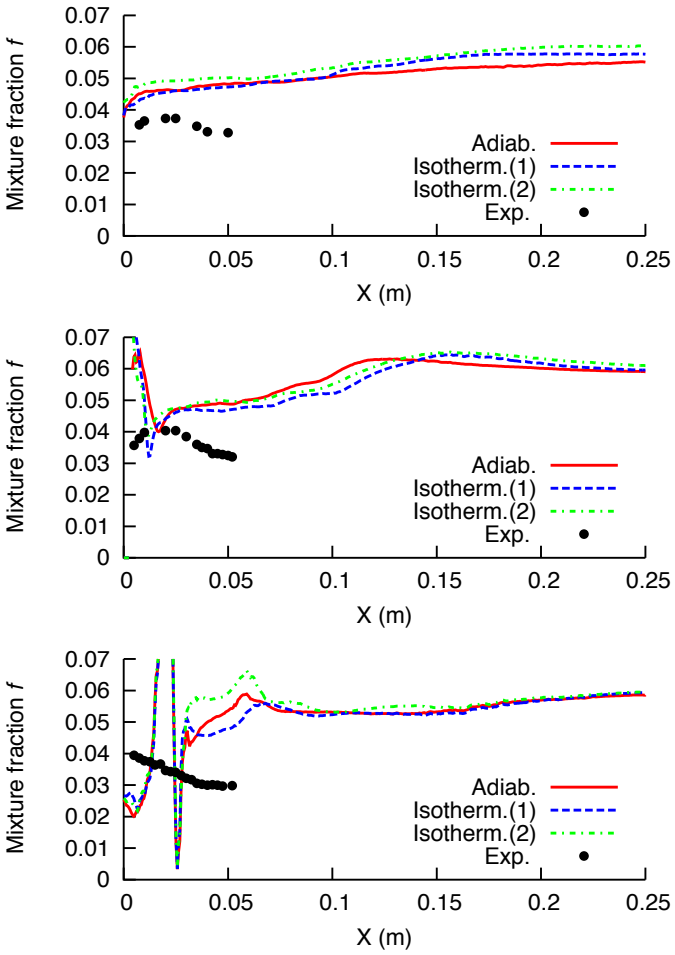

FIGURE 8: ALYA: MIXTURE FRACTION COMPARISON WITH EXPERIMENTAL DATA AT y=0.0m (TOP), y=0.02 m (MIDDLE) and y=0.034m (BOTTOM).

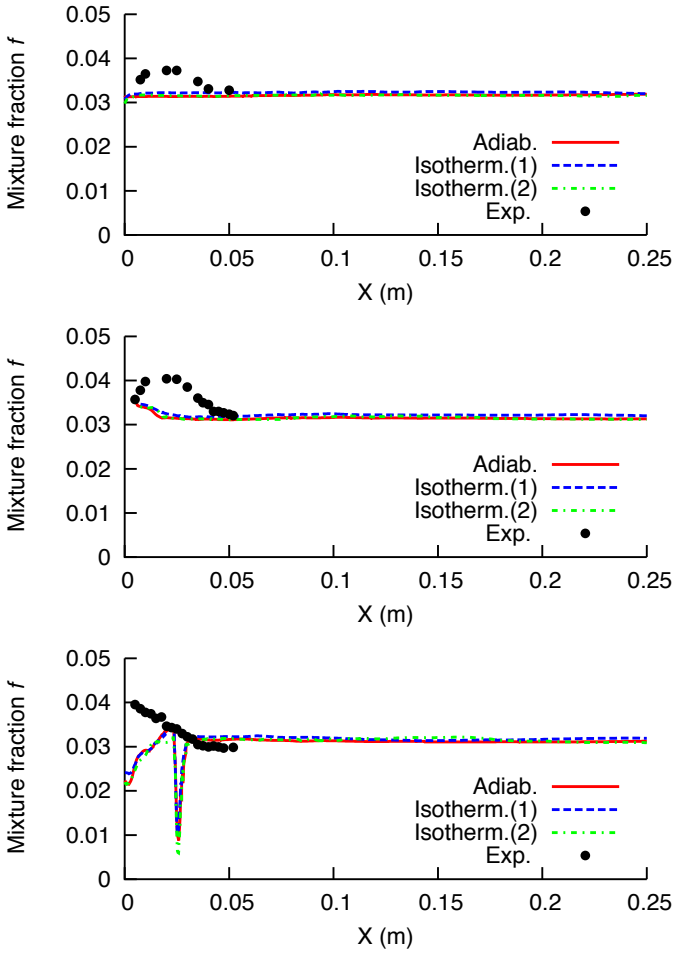

FIGURE 9: OPENFOAM: MIXTURE FRACTION COMPARISON WITH EXPERIMENTAL DATA AT y=0.0m (TOP), y=0.02 m (MIDDLE) and y=0.034m (BOTTOM).

be seen in Fig. 12 where profiles of temperature are compared to the experimental data. As shown by the Alya profiles, despite the over-prediction of temperature due to the wrong mixture fraction field, the adiabatic condition at the wall prevents the formation of temperature variations near the wall and a more uniform profile is found in this case. The second measurement station ($y = 0.02$m) is located across cone, and the correlation increases at this location. At the last measurement point ($y = 0.03$m), where the interaction between the pilot and the main flame occurs, there is a shift in the temperature peak and the code predicts the flame front further downstream.

In OpenFOAM, the overall temperature prediction has an acceptable level of correlation with the experimental data. At the centreline, OpenFOAM over-predicts the temperature close to the igniter, although the correlation improves further downstream. At half way of the cone ($y = 0.02$m), the correlation is improved, but further resolution would be needed in order to capture the temperature peak of the reacting shear layer attached to the wall of the pilot cone. These measurement locations are expected to be influenced by the wall thermal condition. At the last measurement station, OpenFOAM also shifts downstream the peak value of the temperature indicating that the code was not able to capture the flame length correctly in this region.

In general, it is observed that the two codes over-predict the temperature in the central region of the combustor and the fixed temperature of T_w=1000K in the combustor walls has little influence on the mean value of the overall temperature. This indicates that this value of temperature is still too high to be realistic or other heat losses mechanisms such as radiation could also play an important role in this combustor.

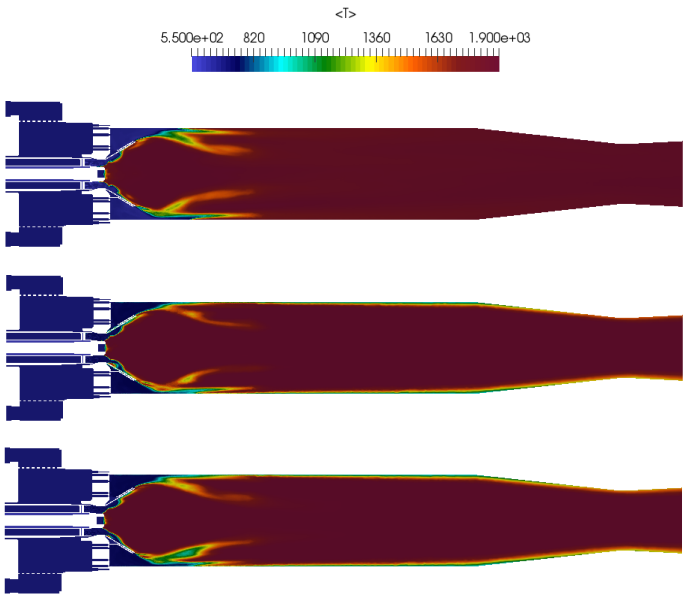

FIGURE 10: TEMPERATURE AT MIDDLE PLANE FOR *ALYA* ADIABATIC (TOP), ISOTHERM.(1) (MIDDLE) AND ISOTHERM.(2) (BOTTOM) CONDITIONS.

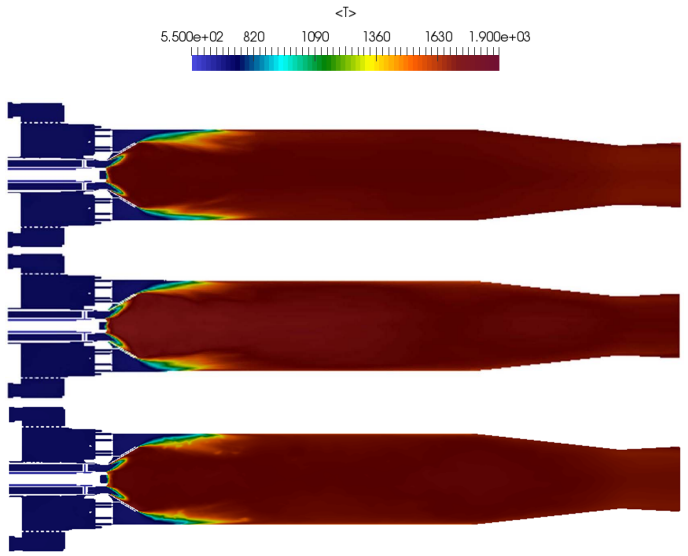

FIGURE 11: TEMPERATURE AT MIDDLE PLANE FOR *OPENFOAM* ADIABATIC (TOP), ISOTHERM.(1) (MIDDLE) AND ISOTHERM.(2) (BOTTOM) CONDITIONS.

CONCLUSIONS AND ONGOING WORK

The downscaled Siemens gas turbine combustor has been simulated with the codes Alya and OpenFOAM using a tabulated chemistry approach in the context of LES. The effect of the thermal boundary conditions at the walls is investigated considering

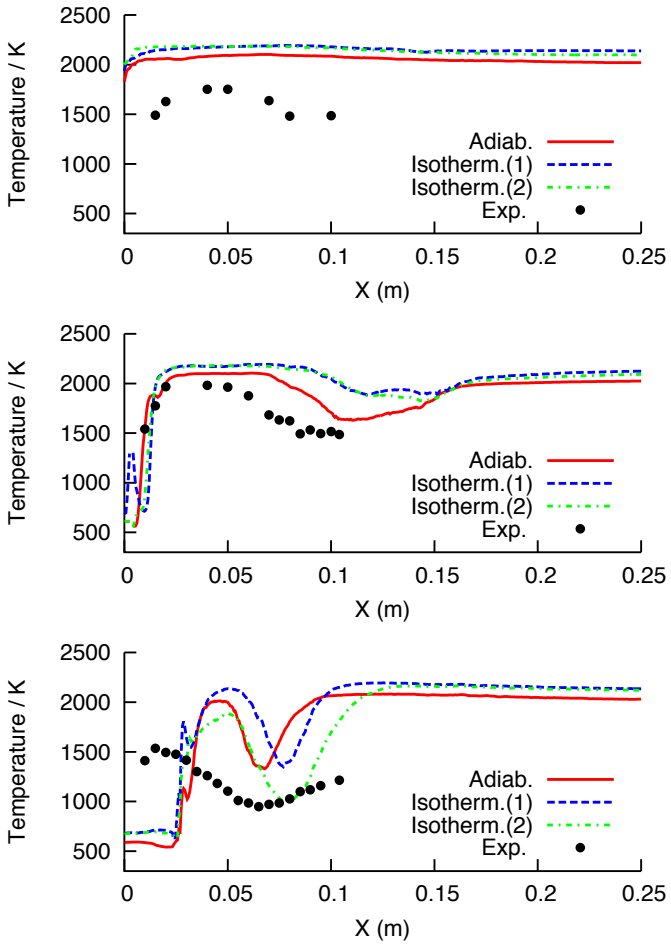

FIGURE 12: ALYA: TEMPERATURE COMPARISON WITH EXPERIMENTAL DATA AT y=0.0m (TOP), y=0.020m (MIDDLE) and y=0.034m (BOTTOM).

adiabatic and isothermal walls. To ensure that the combustion model is able to reproduce results from detailed chemistry, a 1-D laminar flame comparison at the operating conditions of the combustor is performed. Time-averaged axial velocity, mixture fraction and temperature contours from each code are presented and compared with experimental data. Both codes are able to match reasonably well the axial velocity at the recirculation zone. Results from Alya show a significant over-prediction of the mixture faction within the chamber that leads to an over-prediction of temperature causing also a lack of correlation with the velocity measured by the experiments. Results from OpenFOAM for the mixture fraction and temperature are in better agreement with the experimental data, although temperature was over-predicted at the line where the interaction between the pilot and the main flames takes place. Despite the discrepancies with the experimental data, both codes showed the same effect when changing

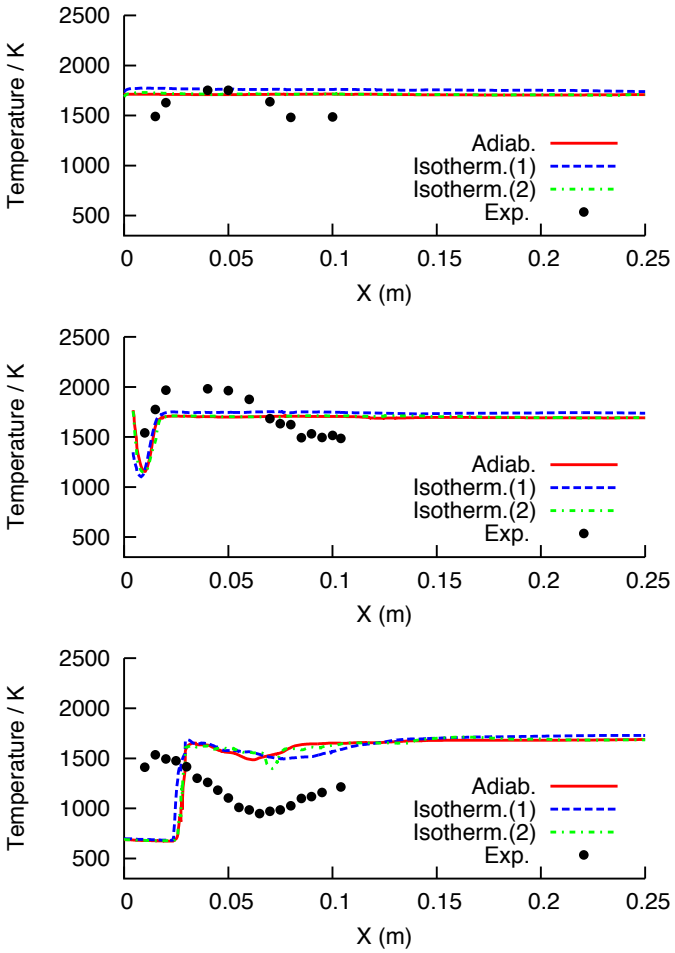

FIGURE 13: OPENFOAM: TEMPERATURE COMPARISON WITH EXPERIMENTAL DATA AT y=0.0m (TOP), y=0.020m (MIDDLE) and y=0.034m (BOTTOM).

the thermal wall conditions. The addition of heat losses by imposing a fixed wall temperature influences some prediction parameters: the main flame was shorter while the temperature in the chamber was higher and the pilot flame was enlarged as heat losses are accounted for. The ongoing work is focused on the analysis and description of the instantaneous fields and the over-prediction of the mixture fraction in Alya code, which has strong influence on the prediction capabilities of the numerical simulations.

ACKNOWLEDGEMENTS

The research leading to these results has received funding through the People Programme (Marie Curie Actions) of the European Union's Seventh Framework Programme (FP7, 2007-2013) under the grant agreement No. FP7-290042 for the project COPA-GT and the European Union's Horizon 2020 Programme (2014-2020) and from Brazilian Ministry of Science, Technology and Innovation through Rede Nacional de Pesquisa (RNP) under the HPC4E Project, grant agreement No. 689772. The authors thankfully acknowledge the computer resources, technical expertise and assistance provided by the Red Española de Supercomputación (RES).